Available online at www.sciencedirect.com
ScienceDirect
Materials and Design 29 (2008) 1330–1333
Materials & Design
www.elsevier.com/locate/matdes

Constitutive equation for superplastic Ti–6Al–4V alloy

G. Giuliano *

Cassino University/Department of Industrial Engineering, via Di Biasio, 43-03043 Cassino (FR), Italy

Received 26 February 2007; accepted 2 July 2007
Available online 18 July 2007

Abstract

Superplasticity is the capability of some materials to exhibit large plastic deformations prior to failure. Structural superplasticity is observed in fine-grained alloys (the average grain size does not exceed 10 μm) under proper conditions of:

- high temperature (greater than about one-half the absolute melting point);
- a controlled strain-rate (within the strain-rate range 10^{-4} to 10^{-2} s^{-1}).

Commercial applications of superplastic forming are restricted to aluminium and titanium alloys. In the aircraft and automotive industries, superplastic forming shows promise as a main approach for producing light, complex-shaped parts.

This paper describes a method to determine the material constants of superplastic alloys from a free forming test at constant pressure. In the finite element simulation the constitutive equation based on power law with hardening variables containing significant physical elements is chosen to fit the true stress, true strain and true strain-rate obtained from experimental data for Ti–6Al–4V at 1200 K. The finite element simulation of the free forming process is used to examine the validity of the suggested method.

Keywords: C. Superplastic forming; F. Material constants; A. Ti–6Al–4 V alloy

1. Introduction

Superplasticity is a capability displayed by some metals and alloys which have a very fine grain structure (the average grain size does not exceed 10 μm) at a temperature greater than about one-half the absolute melting point. These materials exhibit large plastic deformations prior to failure and a very low strength. Elongations ranging from two hundred to several thousand per cent have been obtained [1,2].

At constant temperature, the material sheet is stretched into the die cavity by using a gas under pressure. The load curve is regulated so that the strain-rate induced in the material is kept within the optimum superplastic range (within the strain-rate range 10^{-4} to 10^{-2} s^{-1}). Nowadays, the finite element method (FEM) is the analysis method mainly used to simulate the superplastic forming processes. In [3,4], by the finite element method, two techniques to control the load curve pressure-time in superplastic forming processes have been proposed.

Superplastic behaviour has been demonstrated in several aluminium and titanium alloys. In superplastic aluminium alloys, the required fine grain size can be achieved by two different processes: static or dynamic recrystallization [5]; while the Ti–6Al–4V alloy is superplastic in its conventionally produced state [6]. A summary of some alloys and their related superplastic properties is shown in Table 1 [5,6].

The aerospace and automotive industries have already taken the opportunity of producing complex-shaped products in a limited number of mechanical steps [5,6].

The mechanical behaviour of superplastic materials is normally described by the power-law relationship between the equivalent stress σ, equivalent strain ε and equivalent strain-rate $\dot{\varepsilon}$ as [1,2]:

* Tel.: +353 61 234130; fax: +353 61 202913.
E-mail address: giuliano@unicas.it

0261-3069/$ - see front matter © 2007 Elsevier Ltd. All rights reserved.
doi:10.1016/j.matdes.2007.07.001

Table 1
Comparative properties of superplastic alloys

Alloy	Temperature (K)	Strain-rate (s^{-1})	Elongation %
Al–33%Cu	673–793	8×10^{-4}	400–1000
Al–5%Ca–5%Zn	823	8×10^{-3}	600
Al–6–11%Zn, 1–1.5%Mg, 0.2–0.4%Zr	823	10^{-3}	1500
7475 Al–5.8%Zn–1.6%Cu–2.3%Mg–0.22%Cr	789	2×10^{-4}	800–1200
Supral100 Al–6%Cu–0.4%Zr	723	10^{-3}	1000
Supral220 Al–6%Cu–0.35%Mg–0.1%Ge–0.1%Si	723	10^{-3}	900
Al–2.5%Li–1.2%Cu–0.6%Mg–0.13%Zr	773	3×10^{-3}	800
Ti–6Al–4V	1113–1143	1.3×10^{-4} – 10^{-3}	750–1170
Ti–6Al–5V	1123	8×10^{-4}	700–1100
Ti–6Al–2Sn–4Zr–2Mo	1173	2×10^{-4}	538
Ti–4.5Al–5Mo–1.5Cr	1144	2×10^{-4}	>510
Ti–6Al–4V–2Ni	1088	2×10^{-4}	720
Ti–6Al–4V–2Co	1088	2×10^{-4}	670
Ti–6Al–4V–2Fe	1088	2×10^{-4}	650
Ti–5Al–2.5Sn	1273	2×10^{-4}	420
Ti–15V–3Cr–3Sn–3Al	1088	2×10^{-4}	229

$$\sigma = K\varepsilon^{n}\dot{\varepsilon}^{m} \tag{1}$$

where n is the hardening index, m the strain-rate sensitivity index and K a material constant. This equation is not able to model grain growth kinetics during superplastic deformation and the material hardening due to grain growth. However, the material constants, K, n and m can be obtained by using a simple forming test method. The method consists of subjecting flat metal sheets to constant pressure free bulging processes and determining the data of the dome apex height versus time. Detailed information for the determination of n, m and K is reported in [7].

2. Description of numerical analyses

In the finite element simulation, the mechanical behaviour for the Ti–6Al–4V alloy at 1200 K is characterised by the power-law constitutive equation together with the hardening variables.

The material constants are determined from experimental data obtained by Ghosh and Hamilton [8] using the technique proposed by Lin and reported in [9].

Tensile tests at constant strain-rate (5×10^{-3}, 10^{-3}, 2×10^{-4} and $5\times10^{-5}\,s^{-1}$) were conducted by Ghosh and Hamilton on specimens taken from a single sheet (1.63 mm thick) of Ti–6Al–4V alloy [8]. Three starting grain sizes were utilized in their experimental program. These grain sizes were 6.4, 9.0, and 11.5 μm, respectively [8].

The grain growth rate equation, proposed by Zhou and Dunne in [10] to model grain growth kinetics, contains an isothermal contribution to the grain growth through the index α_1 and a strain-rate dependence through the index β_1, expressed as:

$$\dot{d} = (\alpha_1 + \beta_1\dot{\varepsilon})d^{-\gamma_0} \tag{2}$$

where γ_0 the material constant that indicates the effect of the grain size on the grain growth rate.

The power-law based effective strain-rate $\dot{\varepsilon}$, with hardening variables, can be expressed as:

$$\dot{\varepsilon} = \left(\frac{\sigma - R - k}{K}\right)^{1/m} d^{-\gamma} \tag{3}$$

where γ the hardening index due to grain growth, k the yield stress and R an isotropic hardening variable. The evolution equation of R is given by:

$$\dot{R} = b(Q - R)\dot{\varepsilon} \tag{4}$$

where b and Q are material constants. All details concerning the material constants are reported in [9].

In the finite element analysis, the element type used is a four-node, isoparametric, arbitrary quadrilateral written for axisymmetric applications [11]. The total number of elements is 112, with 226 nodes × 2 degrees of freedom. Since this element uses bilinear interpolation functions, the strains tend to be constant throughout the element. The stiffness of this element is formed using a four-point Gaussian integration. The element has two coordinates in the global z- and r-direction. Due to the symmetry of the geometry, the load and the constraint conditions, only half of the cross-section of the sheet metal was analysed. Moreover, it was necessary to impose constraint conditions on the periphery of the sheet in order to simulate the action of a blank holder.

The properties of the material and the pressure, applied to the top part of the sheet metal, are included using a subroutine. Constant pressures, p, of 0.10 and 0.18 MPa were used in the simulations.

Numerical analyses of free bulging test (Fig. 1) were carried out to validate the proposed method in [7].

3. Results of numerical analyses

Fig. 2 shows the strain-rate evolution and the average grain size versus H at the dome apex. H is defined as the dome height, h, relative to initial radius, a, of the sheet metal (Fig. 1). It can be noted that the induced strain-rate

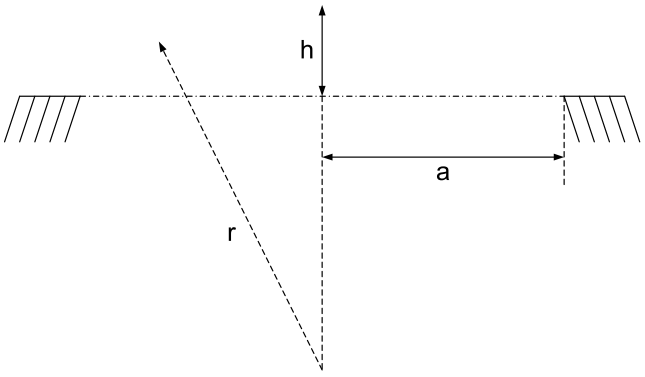

Fig. 1. Scheme of the free bulging test.

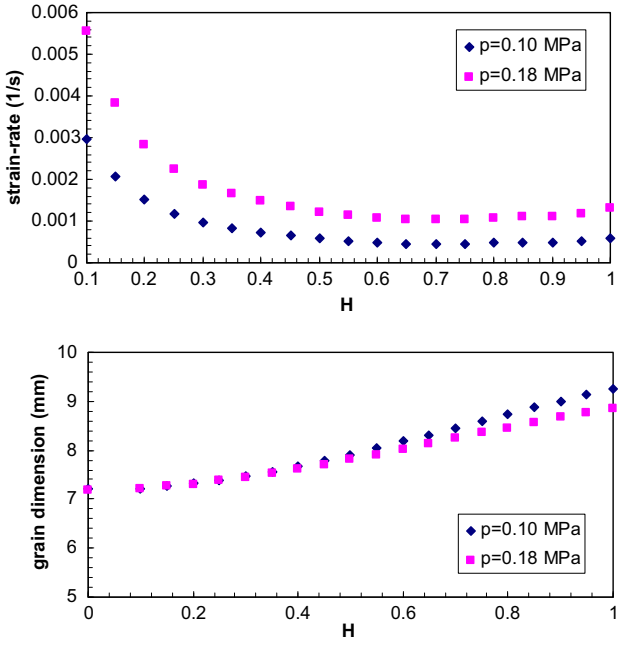

Fig. 2. Evolution of strain-rate and average grain size at dome apex for different pressure values.

at $p = 0.10$ MPa (the minor value of strain-rate is $4.1 \times 10^{-4}\ s^{-1}$) is smaller than the strain-rate induced at the pressure of 0.18 MPa (the minor value of strain-rate is $10^{-3}\ s^{-1}$). Vice versa, the average grain size increases at the smaller pressure since the forming time is higher.

At $H = 1$, for $p = 0.10$ MPa the grain size corresponding to initial grain size of 7.2 μm is 9.27 μm, while for $p = 0.18$ MPa the grain size reaches the value of 8.88 μm.

It is clear from Fig. 3 that non-dimensional thickness at the dome apex is independent of the imposed pressure. Fig. 3 shows the non-dimensional thickness in the sheet at $H = 1$ and for both values of pressure.

The values of m, n and K are calculated by using Eq. (1) as reported in [7].

The strain-rate sensitivity index can be obtained by using:

$$m = \frac{\ln\left(\frac{p_2}{p_1}\right)}{\ln\left(\frac{t_1}{t_2}\right)} \tag{5}$$

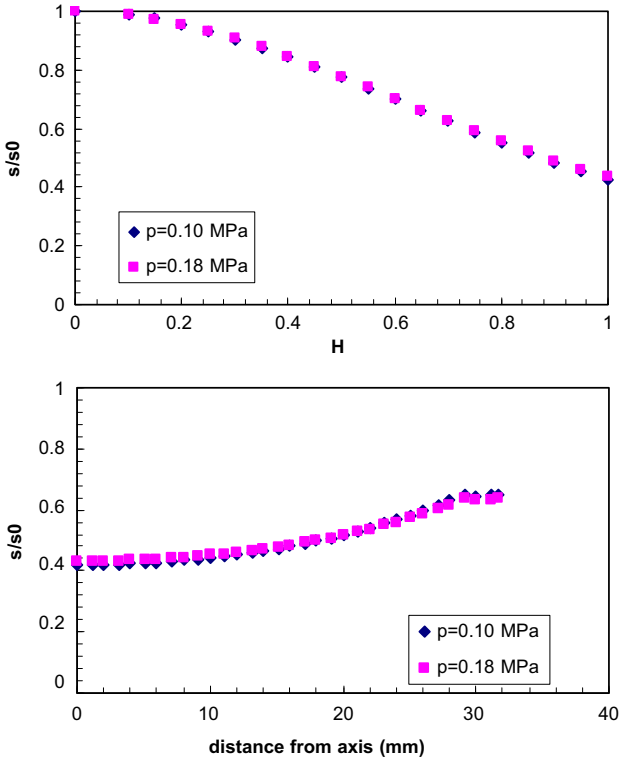

Fig. 3. Evolution of non-dimensional thickness for different pressure values.

This equation was proposed by Enikeev in [12] considering the times t_1 and t_2 at $H = 1$. Fig. 4 shows the strain-rate sensitivity index evolution for different values of H. The average value of m is 0.757, while for $H = 1$ $m = 0.629$. The Enikeev model [12], gave $n = 0$ and $K = 1107.632$, whereas using the model presented in [7] $n = 0.234$ and $K = 3737.259$.

Using the free bulging test two constitutive equations were obtained:

$$\sigma = 3737.259\varepsilon^{0.234}\dot{\varepsilon}^{0.757} \quad \text{for [7]} \tag{6}$$

$$\sigma = 1107.632\dot{\varepsilon}^{0.629} \quad \text{for [12]} \tag{7}$$

Simulations of the forming tests at $p = 0.10$ MPa and $p = 0.18$ MPa were conducted adopting Eqs. (6) and (7).

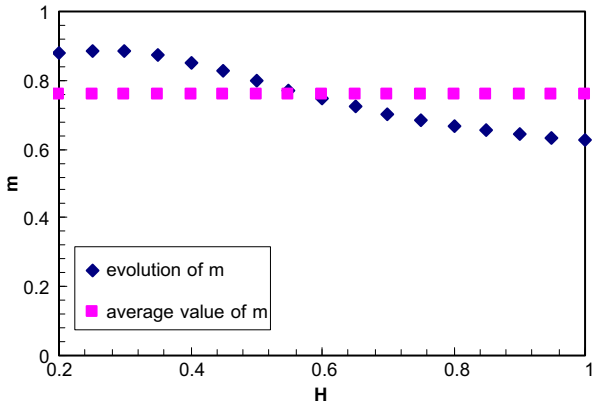

Fig. 4. Evolution of m-value versus H-value.

The Figs. 5 and 6 show the qualitative results predicted by the three models expressed in (3), (6) and (7). It possible to note that: at the pressures $p = 0.10$ and $p = 0.18$ MPa, there is a good agreement between trend of the thicknesses at the dome apex for variations in H obtained by (6) and the results obtained by (3). The maximum error registered in the thickness value is of less than 2%. Vice versa, a comparison between the trends obtained by (3) and (7) shows an error of less than 11% for $H = 1$. Model (7) underestimates the thickness at the dome apex during the forming process. At the pressure $p = 0.18$ MPa, it can be seen that there is a good agreement between the curves of models (3) and (6) with a maximum error of 1%. The curve obtained from (7) lies above the reference one with an error of less than 13% for $H = 1$ (Fig. 5).

At the pressure $p = 0.10$ MPa, the trend of the curve t–H obtained from (6) is close to the curve obtained from (3). Vice versa, the error obtained for $H = 1$ is less than 16% at the pressure $p = 0.18$ MPa. The curve obtained from (7) is above the reference one and has an error of less than 13% for $H = 1$ (Fig. 6).

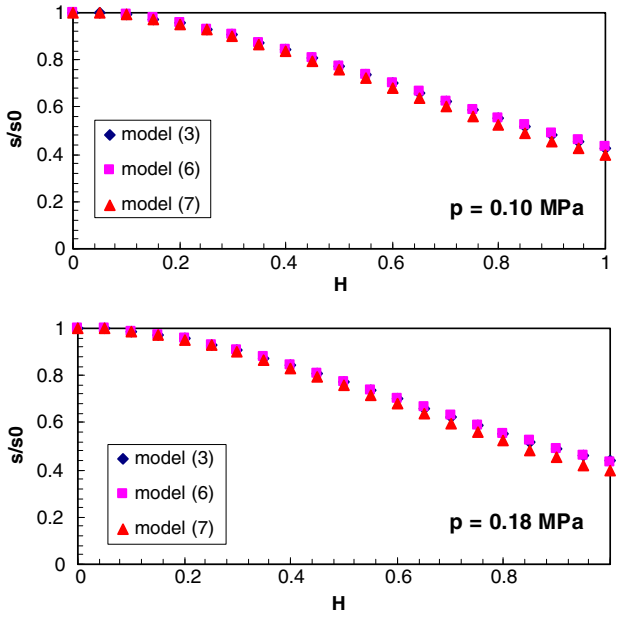

Fig. 5. Comparison between the thicknesses predicted by the three models expressed in Eqs. (3), (6) and (7).

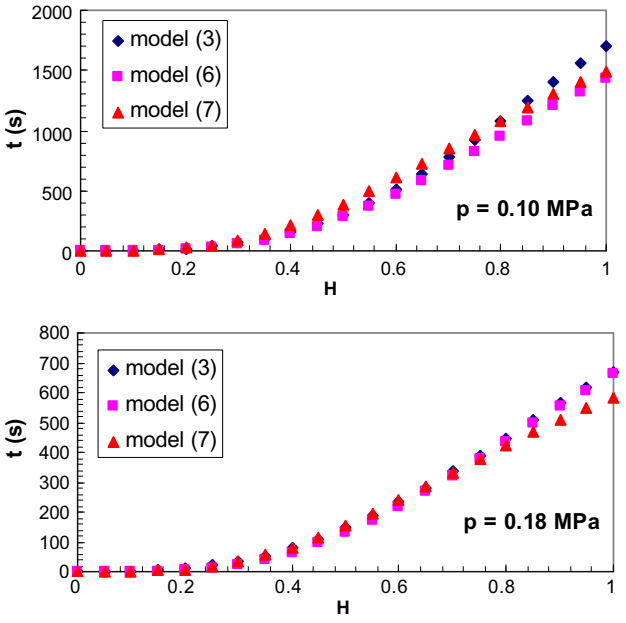

Fig. 6. Comparison between the t–H curves predicted by the three models expressed in Eqs. (3), (6) and (7).

4. Conclusions

Using experimental data from other authors, this study describes an alternative method to the tensile test to determine the material constants of the Ti–6Al–4V superplastic alloy. This is done by means of constant pressure free forming tests. A finite element simulation was carried out to validate the proposed method. The proposed method bears in mind the dependence of flow stress not only on the strain-rate but also on the strain itself.

Acknowledgements

Author wishes to thank the Italian Institutions "Ministero dell'Istruzione, dell'Università e della Ricerca" for financing and supporting the present research activity.

References

[1] C.H. Hamilton, A.K. Ghosh, Superplastic Sheet Forming, in: Metals Handbook, (1988).
[2] Pilling J, Ridley N. Superplasticity in Crystalline Solids. London: The Institute of Metals; 1989.
[3] Carrino L, Giuliano G, Napolitano G. A posteriori optimisation of the forming pressure in superplastic forming processes by the finite element method. Finite Elem Anal Des 2003;39(11):1083–93.
[4] Carrino L, Giuliano G, Palmieri C. On the optimization of superplastic forming processes by the finite element method. J Mater Process Technol 2003;143–144:373–7.
[5] Ghosh AK. Superplasticity in Aluminum Alloys. In: Agrawal SP, editor. Superplastic Forming. The American Society of Metals; 1985. p. 23–42.
[6] Hamilton CH. Superplasticity in Titanium Alloys. In: Agrawal SP, editor. Superplastic Forming. The American Society of Metals; 1985. p. 13–22.
[7] Giuliano G, Franchitti S. On the evaluation of superplastic characteristics using the finite element method. Int J Mach Tool Manu 2006;47:471–6.
[8] Ghosh AK, Hamilton CH. Mechanical behaviour and hardening characteristics of a superplastic Ti–6Al–4V alloy. Metall Trans 1979;10A:699–706.
[9] Lin J. Selection of material models for predicting necking in superplastic forming. Int J Plasticity 2003;19:469–81.
[10] Zhou M, Dunne FP. Mechanism-based constitutive equations for the superplastic behaviour of a titanium alloy. J Strain Anal 1996;31(3):187–96.
[11] MSC. Marc, Theory and user Information, Vol. A, 2005.
[12] Enikeev FU, Kruglov AA. An analysis of the superplastic forming of a thin circular diaphragm. Int J Mech Sci 1995;37/5:473–83.